International Journal of Modern Physics E

$\beta\beta$ DECAY AND NUCLEAR STRUCTURE

E. CAURIER[a], F. NOWACKI[a] AND A. POVES[b]

a) Institut Pluridisciplinaire Hubert Curien
23 rue du Loess BP28 F67037 Strasbourg Cedex, France
b) Departemento de Física Teórica, Universidad Autónoma de Madrid
E-28049 Madrid, Spain

The determination of accurate nuclear matrix elements for $\beta\beta$ decay processes is a challenge for nuclear theory and can have a strong impact in neutrino physics.
Large Scale Shell Model (LSSM) calculations are among the best tools for such determination and recent developments have allowed to extend its application domains. In particular systematic studies of nuclear matrix elements calculations has been now undertaken in this framework for most of the $\beta\beta$ emitters. These calculations are crucial in the determination of the most favorable emitters in the forthcoming generation of $\beta\beta$ experiments. The pesent paper focuses on the recent advances and remaining difficulties of shell model calculations for the neutrinoless mode. Stability and predictive power of the results will be discussed.

1. Introduction

Double beta decay is one of the rarest radioactive decay in nature. It takes place between two even-even isobars when simple β decay is energetically forbidden or strongly hindered by spin mismatch. Several modes can be considered The first decay mode is the two neutrinos mode $(\beta\beta)_{2\nu}$, initialy proposed par Goeppert-Mayer en 1935[2]. This process appears as a second order perturbation theory of the standard model of weak interactions, independently of neutrinos properties. In this two nucleons mechanism, the following decay happens:

$$2n \longrightarrow 2p + 2e^- + 2\bar{\nu},$$

i. e. the decay occurs between isobars(A,Z) and (A,Z+2) via a virtual transition through the intermediate (A,Z+1) nucleus.

Another possible mode is the neutrinoless mode $(\beta\beta)_{0\nu}$. Proposed by Furry in 1939[1], it occurs in the reaction:

$$\begin{aligned} n \longrightarrow p + e^- + \bar{\nu} & \\ \vdots & \\ & \nu \; + n \longrightarrow p + e^- \end{aligned}$$

This decay is forbidden in the standard model since it violates lepton number conservation. Moreover, for such a process, the neutrino has to be its own antiparticle, massive and/or (V+A) weak currents have to be considered. This mode would sensitive to the effective neutrino mass $\langle m_\nu \rangle$. Notice that under certain CP violation conditions, $(\beta\beta)_{0\nu}$ decay can be suppressed. See reference [3] contribution to this workshop proceedings.

Table 1 lists the double beta decay emitters andtheir natual abundancies in nature, with $Q_{\beta\beta}$ larger than natural radioactivity. The challenge for nuclear structure is to try to determine accurately the nuclear matrix elements involved in both decays. Indeed the neutrinoless decay would be charaterized by a total energy of the emitted electrons equalto the $Q_{\beta\beta}$ of the reaction, and would lie in the tail of the continuous spectrum of the two neutrino mode. Favorables cases therefore should have hindered $(\beta\beta)_{2\nu}$ decay and accelerated $(\beta\beta)_{0\nu}$ decay.

Table 1. $\beta\beta$ emitters listed in increasing $Q_{\beta\beta}$ order and their natural abondancies

Transition	$Q_{\beta\beta}$ (keV)	Ab.$(^{232}Th = 100)$
$^{110}Pd \rightarrow ^{110}Cd$	2013	12
$^{76}Ge \rightarrow ^{76}Se$	2040	8
$^{124}Sn \rightarrow ^{124}Te$	2288	6
$^{136}Xe \rightarrow ^{136}Ba$	2479	9
$^{130}Te \rightarrow ^{130}Xe$	2533	34
$^{116}Cd \rightarrow ^{116}Sn$	2802	7
$^{82}Se \rightarrow ^{82}Kr$	2995	9
$^{100}Mo \rightarrow ^{100}Ru$	3034	10
$^{96}Zr \rightarrow ^{96}Mo$	3350	3
$^{150}Nd \rightarrow ^{150}Sm$	3667	6
$^{48}Ca \rightarrow ^{48}Ti$	4271	0.2

2. shell model

Among the possible different tools for matrix elements calculations, shell model is the method of choice since it describes simultaneously all the properties of the low-lying states (deformation and beta decay properties for example) and can be benchmarked on many calculated observables for the surrounding nuclei. The main drawback of shell model approach is in general the difficult tractability of the calculations. Nevertheless a real breakthrough has been achieved in the recent years, (see for example the recent review article [4]) so-called Large Scale Shell Model (LSSM) can be performed and middle mass nuclei like those of table 1 can be investigated in the shell model framework.

Fig. 1. Energy spectrum of the emitted electrons

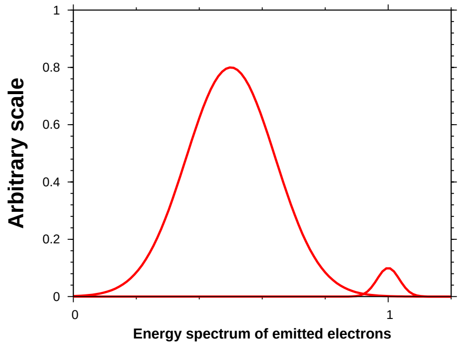

Another advantage of the shell model approach is that the Lanczos Structure Function (LSF) method [5] can be used to determine the low-lying intermediate states involved in the transition decay. Let us recall briefly the sketch of thi method:

If an operator Ω acts on an initial (parent) state $|\Phi_{ini}\rangle$, the resulting state can be expanded in energy eigenstates as:

$$\Omega|\Phi_{ini}\rangle \;=\; \sum_i S(E_i)|E_i\rangle \tag{1}$$

$S(E_i)$ amplitudes being the stucture (or strength) function of the operator Ω. Starting a Lanczos diagonalization procedure using $\Omega|\Phi_{ini}\rangle$ as the initial Lanczos vector allows to get the overlap (therefore $S(E_i)$'s) of this vector with the enregy eigenstates (see reference [4] for details).

The validity and convergence of this approximation is shown in figure 2. On the top panel is shown the Gamow-Teller structure function of ^{48}Ca after 50 and 9470 (full space) Lanczos iterations. The shapes somehow do not appear similar to each other, in the mid-energy range. On the bottom panel the same structure functions are considered but each peak is enlarged with a simulated experimental width. The shapes are now identical and only a few Lanczos iterations are needed to recover the necessary decay information. This powerful method will be used in the following section for the determination of 2ν matrix elements.

3. 2ν calculations

The half-life of the 2ν process is expressed as followed

$$[T^{2\nu}_{1/2}]^{-1} = G_{2\nu}|M^{2\nu}_{GT}|^2, \tag{2}$$

with

$$M^{2\nu}_{GT} = \sum_m \frac{\langle 0^+_f||\vec{\sigma}t_-||1^+_m\rangle\langle 1^+_m||\vec{\sigma}t_-||0^+_i\rangle}{E_m + E_0} \tag{3}$$

$G_{2\nu}$ contains phase space and the axial coupling constant g_A. $G_{2\nu}$ scales like $Q^{11}_{\beta\beta}$ and typical observed half-lives range in $10^{19} - 10^{23}$ years.

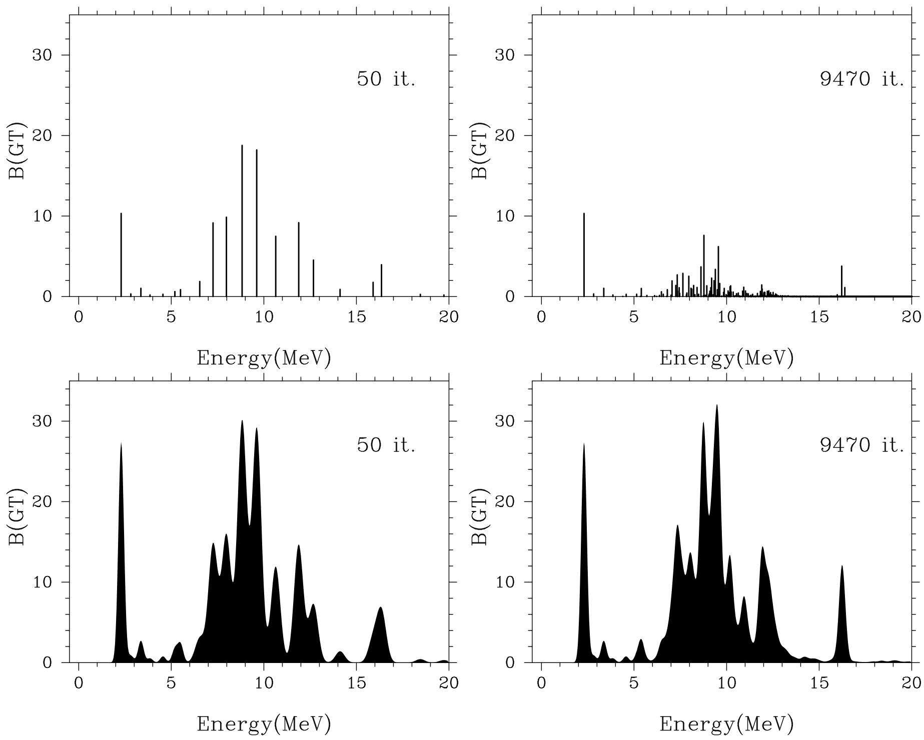

Fig. 2. $^{48}Ca \longrightarrow ^{48}Sc$ Gamow-Teller structure function evolution with Lanczos iterations

The matrix elements calculations requires the explicit summation over all the intermediate 1^+_m states in the (A,Z+1) nucleus. This summation is obtained with the LSF method which allows to obtain a very good approximation of the $(\beta\beta)_{2\nu}$ strength function. The procedure can be divided in four steps:

- calculation of the final $|0^+_f\rangle$ and initial $|0^+_f\rangle$ states
- generatation of the doorway states $\vec{\sigma}t_-|0^+_i\rangle$ and $\vec{\sigma}t_+|0^+_f\rangle$
- use of a doorway in a Lanczos Strength Function method: at iteration N, N 1^+ states are generated in the intermediate nucleus, with excitation energies E_m
- overlap with the other doorway, enter energy denominators and add up the N contributions

One proceeds till convergence is reached. This approximation is enforced by the energy dependance denominator which hinders higher-lying states contributions to the matrix element. Examples of such strength functions are shown in Figure 3. One should notice the positive or negative contributions of the intermediate states in opposite to the single β case.

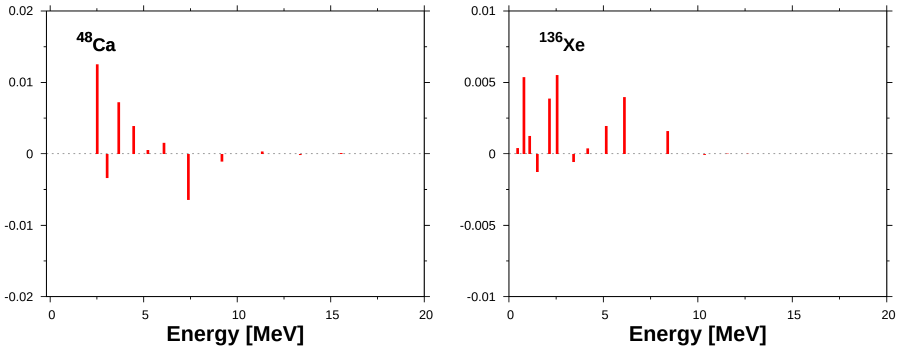

Fig. 3. 2ν strength function in ^{48}Ca and ^{136}Xe

Table 3 shows calculated $T^{2\nu}_{1/2}$ half-lives in several cases for ground-state to ground-state decay. The quenching factor renormalizing the Gamow-Teller operator to $(\sigma\tau)_{eff.}$ has been also used in the double beta case. This factor amounts to 0.744 for ^{48}Ca, ^{76}Ge and ^{82}Se and to 0.57 for ^{130}Te and ^{136}Xe.
The agreement is excellent in all cases and evidently give confidence in the approach

Table 2. Calculated and measured 2ν half-lives for several emitters

Parent nuclei	^{48}Ca	^{76}Ge	^{82}Se	^{130}Te	^{136}Xe
$T^{2\nu}_{1/2}(g.s.)$ th.	$3.7E19$	$1.15E21$	$3.4E19$	$4E20$	$6E20$
$T^{2\nu}_{1/2}(g.s.)$ exp	$4.2E19$	$1.4E21$	$8.3E19$	$2.7E21$	$> 8.1E20$

and the calculated wavefunctions. Nevertheless, one should stress that 2ν and 0ν modes are driven byy completely different operators and that reliable 2ν ME could not implicitely guarantee reliable 0ν ME as often stated in QRPA calculations.

4. 0ν calculations

For the 0ν mode, we will only consider exchange of light neutrinos and only left-handed currents (more sophisticated extension of the standard model can be invoked, with exchange of a massive Higgs particle , the majoron). Under such assumptions, the half-life of the 0ν process is expressed as followed

$$[T^{0\nu}_{1/2}(0^+ \rightarrow 0^+)]^{-1} = G_{0\nu}|M^{0\nu}|^2\langle m_\nu\rangle^2 \tag{4}$$

where $\langle m_\nu\rangle$ is the effective neutrino mass and $G_{0\nu}$, the kinematic phase factor. $G_{0\nu}$ goes like $Q^5_{\beta\beta}$ and therefore, 0ν half-lives are much longer than 2ν ones. The actual lower experimental limit is in the range of 10^{25} years.

The summation over all the intermediate states, a poor approximation in the two neutrinos mode is here a good one since the energy denominators are almost constant due to the average energy of the virtual neutrino of about 100 MeV. Within the closure approximation the operator $M^{(0\nu)}$ to calculate is

$$\langle 0_f^+ || M_K^{(0\nu)} || 0_i^+ \rangle \text{ with } M_K^{(0\nu)} \;=\; \sum_{ijkl} W_{ijkl}^{\lambda,K} \left[(a_i^\dagger a_j^\dagger)^\lambda (\tilde{a_k} \tilde{a_l})^\lambda \right]^K \tag{5}$$

We are left with a standard nuclear structure problem.
$M_K^{(0\nu)}$ can be approximated by two matrix elements of Gamow-Teller and Fermi types:

$$\begin{aligned} M^{(0\nu)} = M_{GT}^{(0\nu)} - \tfrac{g_V^2}{g_A^2} M_F^{(0\nu)} &= \langle 0_f^+ | \textstyle\sum_{n,m} h(\sigma_n . \sigma_m) t_{n-} t_{m-} | 0_i^+ \rangle \\ &- \tfrac{g_V^2}{g_A^2} \langle 0_f^+ | \textstyle\sum_{n,m} h t_{n-} t_{m-} | 0_i^+ \rangle \end{aligned} \tag{6}$$

4.1. *update of* 0ν *nuclear matrix elements calculations*

Table 4.1 shows an update of recently calculated 0ν nuclear matrix elements. Effective neutrino masses $\langle m_\nu \rangle$ are given assuming a decay half-life of 10^{25} years. This table compiles calculations for a set of nuclei requiring a considerable amount of work since they involved different valence spaces and consequently different effective interactions to be determined and tested in the neighbouring nuclei. ^{96}Zr and ^{100}Mo results do not yet appear in this table but should be available in a short future. The valence space for these nuclei is not easy to determine since both nuclei lie in a transitional region between sphericity and strong deformation. The case of ^{150}Nd although mentionned in the table is out of present computational possibilities due to its large deformation. Among the calculated decays, ^{116}Cd seem to be the most favorable case. More generaly spherical cases (where both parent and daughter nuclei exhibit the same spherical shapes) appear to generate large matrix elements. This trend will be commented in the last section of the paper.

4.2. *sensitivity of matrix elements on the effective interaction*

The obtained results depend only weakly on the effective interactions provided they are compatible with the spectroscopy of the region. For the lower pf shell we have three interactions that work properly, KB3, FPD6 and GXPF1. Their predictions for the 2ν and the neutrinoless modes are quite close to each other as shown in Table 4.2.

4.3. *sensitivity of matrix elements on deformation and spin-orbit partners*

Changing adequately the effective interaction we can increase or decrease the deformation of parent, grand-daughter or both, and so gauge its effect on the decays. A mismatch of deformation can reduce the $\beta\beta$ matrix elements by factors 2-3. In

Table 3. Update of 0ν nuclear matrix elements calculations

	$\langle m_\nu \rangle$ for $T_{\frac{1}{2}} = 10^{25}$ y.	$M_{0\nu}^{GT}$	1-χ_F
^{48}Ca	0.85	0.67	1.14
^{76}Ge	0.90	2.35	1.10
^{82}Se	0.42	2.35	1.10
^{96}Zr			
^{100}Mo			
^{110}Pd	0.67	2.52	1.16
^{116}Cd	0.24	2.59	1.19
^{124}Sn	0.45	2.11	1.13
^{128}Te	1.92	2.36	1.13
^{130}Te	0.35	2.13	1.13
^{136}Xe	0.41	1.77	1.13
^{150}Nd			

Table 4. Sensitivity of 0ν ME on the effective interaction

	KB3	FPD6	GXPF1
$M_{GT}(2\nu)$	0.083	0.104	0.107
$M_{GT}(0\nu)$	0.667	0.726	0.621

fact the fictitious decay Ti-Cr, using the same energetics that in Ca-Ti, has matrix elements more than twice larger. If we increase the deformation in both Ti and Cr nothing happens. On the contrary, if we reduce the deformation of Ti, the matrix elements are severely quenched. The effect of deformation is therefore quite important and cannot be overlooked

Similarly, we can increase artificially the excitation energy of the spin-orbit partner of the intruder orbit. Surprisingly enough, this affects very little the values of the matrix elements, particularly in the neutrinoless case. Even removing the spin-orbit partner completely produces minor changes.

As a last point of analysis is shown in Figure 4.3 the contribution to the Gamow-Teller matrix element of the different J components of the $\beta\beta$ hamiltonian. Two

Table 5. Sensitivity of 0ν ME on deformation and spin-orbit partner

	^{48}Ca $\rightarrow^{48}$Ti	^{48}Ti $\rightarrow^{48}$Cr
$M_{GT}(2\nu)$	0.083	0.213
$M_{GT}(0\nu)$	0.667	1.298

Without spin-orbit partner

	^{48}Ca $\rightarrow^{48}$Ti	^{48}Ti $\rightarrow^{48}$Cr
$M_{GT}(2\nu)$	0.049	0.274
$M_{GT}(0\nu)$	0.518	1.386

leading contributions arise from $J = 0$ and $J = 2$ components, with opposite signs. One can now more easily interpret the trend in Table 4.1 favoring spherical parent and daugther nuclei: the wavefunctions of these nuclei are dominated by seniority 0 components which cannot therefore interfer with non-seniority 0 contributions. In the semi-magic cases of ^{48}Ca and ^{136}Xe, this behaviour is not observed since the strong sphericity of the parent nuclei precisely interfers with non-zero seniority components of the daughter nucleus.

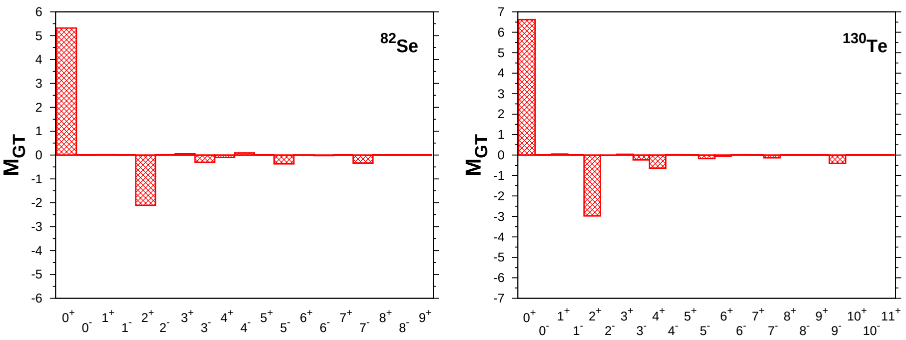

Fig. 4. J-components (particle-particle representation) contributions to the 0ν GT matrix element

5. summary

Large scale shell model calculations with high quality effective interactions are available or will be in the immediate future for all but one of the neutrinoless double beta emitters. The theoretical spread of the values of the nuclear matrix elements entering in the lifetime calculations is greatly reduced if the ingredients of each calculation are examined critically and only those fulfilling a set of quality criteria are retained. A concerted effort of benchmarking between LSSM and QRPA practitioners would be of utmost importance to increase the reliability and precision of the nuclear structure input for the double beta decay processes.

References

1. W. H. Furry Phys. Rev. **56** (1939) 1184.
2. M. Goeppert-Mayer Phys. Rev. **48** (1935) 512.
3. M. Godz and W. Kaminski
   Suppression of the $0\nu2\beta$ decay from CP violation,
   Proceedings of the same workshop
4. E. Caurier, G. Martinez-Pinedo, F. Nowacki, A. Poves, A. P. Zuker
   Rev. Mod. Phys. **77** (2005) 427.
5. Whitehead R. R. in Moment Methods in Many Fermion Systems,
   edited by B. J. Dalton, S. M. Grimes, J. D. Vary, and S. A. Williams
   (Plenum, New York) 1980, p.235.